Mater. Res. Soc. Symp. Proc. Vol. 891 © 2006 Materials Research Society 0891-EE01-11

Structural Defects in InSb Quantum Wells Grown on GaAs (001) Substrates via $Al_{0.09}In_{0.91}Sb$/GaSb-AlSb Strained Layer Superlattice/AlSb/GaSb Buffer Layers

T.D. Mishima, M. Edirisooriya and M.B. Santos
Homer L. Dodge Department of Physics and Astronomy, and
Center for Semiconductor Physics in Nanostructures
University of Oklahoma,
Norman, OK 73019-2053, U.S.A.

ABSTRACT

Structural defects in InSb quantum well (QW) samples have been investigated by transmission electron microscopy (TEM). Using molecular beam epitaxy, an InSb QW with remotely-doped $Al_{0.09}In_{0.91}Sb$ barriers was grown on a GaAs (001) substrate with buffer layers consisting of, in order from the substrate: 1 μm of GaSb, 1 μm of AlSb, 50 nm of GaSb-AlSb strained layer superlattice (SLS), and 3 μm of $Al_{0.09}In_{0.91}Sb$. Cross-sectional TEM analysis indicates that high densities of threading dislocations (TDs) are created at the two highly lattice-mismatched interfaces, the $Al_{0.09}In_{0.91}Sb$/GaSb-AlSb SLS and the GaSb/GaAs interfaces. Pairs of stereo images taken from plan-view TEM (PV-TEM) specimens show that TDs propagate through the InSb QW layer. The densities of TDs and micro-twin (MT) defects measured by PV-TEM are 9×10^8 /cm^2 and 4×10^3 /cm, respectively. These values are worse than those in an InSb QW layer grown with a different buffer layer by a factor of ~4. The different buffer layer contains an InSb interlayer that effectively filters out both TDs and MTs. Adopting an interlayer structure and reducing the GaSb and AlSb layer thickness may make it possible to fabricate a lower-defect-density yet thinner InSb QW sample with the type of buffer layer examined in this study.

INTRODUCTION

Electrons in InSb have a high electron mobility, a large effective *g* factor and strong spin-orbit effects [1]. Ongoing efforts are being made to develop InSb quantum well (QW) -based devices that take advantage of these properties, such as field effect transistors [2], mesoscopic magnetoresistors [3], ballistic transport devices [4] and spin transport devices. One key factor to improve the performance of such devices is the minimization of structural defects. Since there are no lattice-matched III-V substrates that are also semi-insulating, InSb QW structures are usually grown on semi-insulating GaAs (001) substrates in spite of the large lattice mismatch of 14.6% between InSb and GaAs. Efforts have been made to optimize the buffer layers for both InSb QW structures [5] and InSb epilayers [6-8] grown on GaAs (001). Recently, studies using transmission electron microscopy (TEM) and Hall effect measurements showed that the density of micro-twins (MTs) correlates with the electron mobility in the InSb QW layer [9-11]. When a MT passes through an InSb QW layer, it causes 1) an offset between the two parts of the QW bisected by the MT, 2) a different crystallographic orientation of the QW in the MT region, 3) bending in the QW near the MT and, 4) formation of a wall of aligned threading dislocations (TDs) which propagate along the MT [9-11].

In this study, we report additional TEM observations of structural defects in an InSb QW structure grown on a GaAs (001) substrate. The buffer layer deposited between the QW structure and the substrate consists of $Al_{0.09}In_{0.91}Sb$, GaSb-AlSb strained layer superlattice (SLS), AlSb, and GaSb layers. This is one of the buffer layer structures we evaluated when searching for an effective defect filtering technique for this system, which turned out to be the insertion of an InSb interlayer between two $Al_{0.09}In_{0.91}Sb$ layers, as reported previously [5]. Cross-sectional TEM (X-TEM) images show that high densities of TDs are created at the two high lattice-mismatch interfaces, the GaSb/GaAs interface and the $Al_{0.09}In_{0.91}Sb$/GaSb-AlSb SLS interface. TDs cutting through the InSb QW layer are clearly imaged by a stereo-imaging technique taken in a plan-view TEM (PV-TEM) geometry. The TD and MT densities measured by PV-TEM are 9×10^8 /cm^2 and 4×10^3 /cm, respectively. These values are about 4 times higher than in an InSb QW sample that included an InSb interlayer in a different buffer layer that was 14% thinner. Based on these TEM observations, two ways to improve the type of buffer layers examined in this study are proposed: 1) inserting an InSb interlayer in the $Al_{0.09}In_{0.91}Sb$ layer and 2) reducing the thickness of GaSb and AlSb layers located under the GaSb-AlSb SLS/$Al_{0.09}In_{0.91}Sb$ interface.

EXPERIMENTAL DETAILS

An InSb QW sample was grown in an Intevac GEN-II molecular epitaxy system. A quarter of a 3-inch semi-insulating GaAs (001) wafer was used as a substrate. The substrate was pre-heated at 375°C for 20 hours. Oxide desorption from the substrate surface was made at 650°C. The buffer layer, starting from the substrate surface, was 1 μm of GaSb grown at 480°C, 1 μm of AlSb grown at 530°C, a 50 nm GaSb-AlSb SLS grown at 530°C, and 3 μm of $Al_{0.09}In_{0.91}Sb$ grown at 400°C. The SLS was composed of 10 periods of 2.5 nm GaSb and 2.5 nm AlSb. On top of the buffer layer, an InSb QW structure was grown at 320°C at a rate of ~1 μm/hr. It consisted of a Si δ- doping layer (to supply electrons to the QW), a 60 nm $Al_{0.09}In_{0.91}Sb$ lower barrier layer, a 30 nm InSb QW layer, a 60 nm $Al_{0.09}In_{0.91}Sb$ upper barrier layer, a Si δ-remotely doping layer (to supply electrons to the QW), a 100 nm $Al_{0.09}In_{0.91}Sb$ layer, a Si δ- doping layer (to supply electrons to surface states), a 10 nm $Al_{0.09}In_{0.91}Sb$ layer and a 10 nm InSb cap layer. More details about this type of InSb QW structure can be found elsewhere [5,9]. A 10 sec growth interrupt was executed when hetero-interfaces were formed. Reflection high energy electron diffraction patterns from the substrate surface were streaky throughout the entire growth, except when the GaSb/GaAs interface was formed. Van der Pauw measurements show that the QW structure has a Hall electron mobility of 26,000 cm^2/Vs with a carrier density of 7.2×10^{11} /cm^2 at room temperature.

The sample was characterized using a JEOL JEM-2000FX TEM operated at an acceleration voltage of 200kV. Both X-TEM and PV-TEM specimens were made out of the samples by mechanical thinning, dimpling and ion milling. For PV-TEM specimens, these processes were done from the back side so that the top part of the samples could be observed by TEM. Therefore, when a PV-TEM specimen has a thickness of more than 210 nm, it includes an InSb QW layer which is located between 180 and 210 nm below the sample surface. To minimize damage, the specimens were cooled down using liquid nitrogen during the ion milling process.

RESULTS AND DISCUSSIONS

Figures 1(a) and 1(b) show X-TEM images for the middle part (the 3 μm $Al_{0.09}In_{0.91}Sb$ layer, 50 nm GaSb-AlSb SLS, and 1 μm AlSb layer) and the bottom part (the 1 μm AlSb layer, 1 μm GaSb layer, and GaAs (001) substrate) of the sample, respectively. These images were taken under a dark field (DF) condition with the 220 reflection. Most of the thin line contrasts in the figures derive from dislocations. Misfit dislocations (MDs) are visible in figure 1(b) at the interface between the GaSb layer and the GaAs substrate where the lattice mismatch is 7.8%. Around this interface, TDs that propagate toward the sample surface are nucleated. The number of TDs appears to decrease as the GaSb layer thickness increases, presumably due to annihilations and reactions among the TDs. Other bunches of MDs are formed at the AlSb/GaSb interface where the lattice mismatch is 0.7%. Some TDs appear to be bent and change into MDs at the interface, leading to the decrease in the number of TDs. The number, however, increases drastically above the $Al_{0.09}In_{0.91}Sb$/GaSb-AlSb SLS interface, as shown in figure 1(a). The lattice constant at the top region of the SLS is estimated to be between 0.6136 nm (AlSb) and 0.6094 nm (GaSb), due to a possible lattice relaxation in the SLS. Therefore, the lattice mismatch at the $Al_{0.09}In_{0.91}Sb$/GaSb-AlSb SLS interface is between 5.1% and 5.8%. The number of TDs in the $Al_{0.09}In_{0.91}Sb$ layer decreases as they propagate toward the sample surface.

Figure 2(a) is a PV-TEM image taken under a bright-field imaging condition. The direction of the electron beam was set to be parallel to the <001> direction. In addition to thin-line dislocation contrasts, a rectangular contrast that derives from a MT [9-11] is seen at the bottom of the image. Since a MT is located in the {111} plane which is tilted by 54.7° with respect to the (001) sample surface, the specimen thickness, t, can be estimated by a simple equation, $t = w \times \tan 54.7°$, where w is the width of a MT in a <001>-directional PV-TEM image such as figure

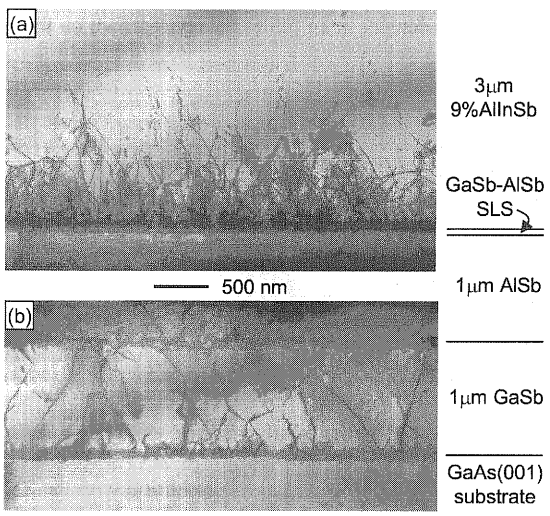

Figure 1. Cross-sectional TEM images for a) the middle part and b) the lower part of the InSb QW sample. High densities of TDs are created around and the $Al_{0.09}In_{0.91}Sb$/GaSb-AlSb SLS and the GaSb/GaAs interfaces.

2(a). The width of the MT in figure 2(a) is measured to be ~150 nm, indicating that the specimen thickness is ~212 nm. Since the bottom of the InSb QW layer is 210 nm below from the top of the sample surface, the specimen should include the QW layer and the layers above it.

In order to examine the relation between the dislocations and the InSb QW layer in figure 2(a), we used stereo imaging technique for the same area of the specimen. Figures 2(b) and 2(c) show a pair of stereo PV-TEM images which enable us to take a look at the dislocations in a three-dimensional space. These images were taken under a DF image condition with the 220 reflection. In the thee-dimensional image, most of the dislocations are seen to cut through the specimen diagonally from the bottom to the top, indicating that they are TDs. Since the specimen thickness is ~212nm, the TDs are cutting through the InSb QW layer.

PV-TEM measurements show that the densities of TDs and MTs are 9×10^8 /cm^2 and 4×10^3 /cm, respectively, in the InSb QW structure grown on the 5.05 μm-thick buffer layer. We have already reported a lower-defect-density InSb QW structure (TD density = 2×10^8 /cm^2 and MT density = 1×10^3 /cm) that can be made with a different, thinner (4.34 μm) buffer layer that consists of, starting from the substrate surface, 130 nm of GaAs, 1 μm of AlSb, 10 nm of GaSb, 1 μm of $Al_{0.09}In_{0.91}Sb$, 200 nm of InSb, and 2 μm of $Al_{0.09}In_{0.91}Sb$ on a GaAs (001) substrate [5]. Although both samples have a similar overall lattice constant change of 0.5653 nm (GaAs) → ~0.61 nm (AlSb and GaSb) → ~0.65 nm ($Al_{0.09}In_{0.91}Sb$ and InSb) from the substrate to the InSb QW structure, there are differences both in details of the buffer layer structures and in the growth conditions. This makes it difficult to deduce straightforwardly the reasons for the defect density differences between these two samples. However, we believe that the 200 nm InSb layer in the better sample plays an important role. TEM analysis has revealed that the interfaces between InSb and $Al_{0.09}In_{0.91}Sb$ layers are very effective in filtering out both TDs and MTs [5,9]. The type of buffer layer examined in this study includes a 3 μm layer of $Al_{0.09}In_{0.91}Sb$ where an InSb interlayer can be added. We believe that the insertion of an InSb interlayer will make it possible to obtain a lower defect density in an InSb QW layer grown on the type of buffer layer examined in this study.

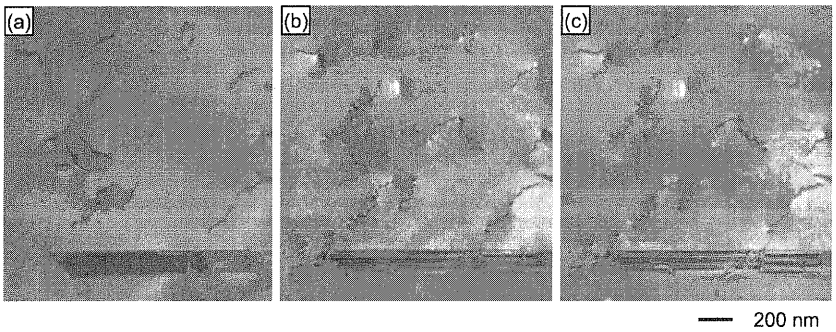

Figure 2. a) Plan-view TEM images taken under <001> on-axis bright-field imaging condition. A rectangular contrast at the bottom of the image derives from a micro-twin. b) and c) a pair of stereo images taken under dark-field imaging condition with the 220 reflection. By looking at b) and c) with left and right eyes, respectively, one can see that threading dislocations propagate through the specimen in a 3D space. Putting a piece of paper vertically between b) and c) may help to see the 3D image. Steeply inclined threading dislocations exhibit a zigzag line contrast under the image condition used for these images [12].

Additional improvement of the buffer layer may be possible by reducing the thickness of the GaSb and AlSb layers that are located below the GaSb-AlSb SLS/$Al_{0.09}In_{0.91}Sb$ interface. As shown in figures 1(a) and 1(b), although the number of TDs created at the GaSb/GaAs interface decreases as the GaSb and AlSb layer thicknesses increase, it increases significantly at the $Al_{0.09}In_{0.91}Sb$/GaSb-AlSb SLS interface. If this increase in TDs is not strongly dependent on the number of pre-existing TDs in the AlSb layer, it may be possible to make a thinner InSb QW sample with thinner GaSb and AlSb layers, which would still have an almost equivalent TD density in the InSb QW layer.

CONCLUSIONS

In summary, transmission electron microscopy (TEM) was used to investigate structural defects in an InSb quantum well (QW) sample grown on a GaAs (001) substrate. Cross-sectional TEM images showed that the initial site for creation of a high density of threading dislocations (TDs) is around the GaSb/GaAs interface. Although the number of TDs appears to decrease with increasing the GaSb and AlSb layer thicknesses, the creation of another high density of TDs occurs around the second preferential site, the $Al_{0.09}In_{0.91}Sb$/GaSb-AlSb SLS interface. The number of newly created TDs also decreases as the $Al_{0.09}In_{0.91}Sb$ layer thickness increases. Stereo images taken under plan-view TEM condition allowed us to deduce that TDs as well as micro-twins (MTs) cut through the InSb QW layer. The densities of TDs and MTs are 9×10^8 /cm^2 and 4×10^3 /cm, respectively. By comparing these TEM data with those obtained from an InSb QW sample with fewer defects, two ways to improve the type of buffer layer examined in this study are suggested: 1) incorporating a defect-filtering InSb interlayer into the $Al_{0.09}In_{0.91}Sb$ buffer layer and 2) reducing the GaSb and AlSb layer thicknesses.

ACKNOWLEDGMENTS

The authors would like to thank K.J. Goldammer for designing and growing the samples and J.C. Keay and G.W. Strout for technical assistance. They also gratefully acknowledge use of the Samuel Roberts Noble Electron Microscopy Laboratory of the University of Oklahoma. This work was partly supported by the NSF under Grants Nos. DMR-0520550 and DMR-0510056.

REFERENCES

1. G.A. Khodaparast, R.E. Doezema, S.J. Chung, K.J. Goldammer, and M.B. Santos, Phys. Rev. B **70**, 155322 (2004).
2. T. Ashley, A.R. Barnes, L. Buckle, S. Datta, A.B. Dean, M.T. Emeny, M. Fearn, D.G. Hayes, K.P. Hilton, R. Jefferies, T. Martin, K.J. Nash, T.J. Phillips, W.H.A. Tang, P.J. Wilding, and R. Chau, The 7th International Conference on Solid-State and Integrated Circuit Technology (2004).
3. S.A. Solin, D.R. Hines, A.C.H. Rowe, J.S. Tsai, Yu.A. Pashkin, S.J. Chung, N. Goel, and M.B. Santos, Appl. Phys. Lett. **80**, 4012 (2002).

4. N. Goel, S.J. Chung, M.B. Santos, K. Suzuki, S. Miyashita, and Y. Hirayama, Physica E **21**, 716 (2004).
5. T.D. Mishima and M.B. Santos, J. Vac. Sci. Technol. B **22**, 1472 (2004).
6. L.K. Li, Y. Hsu, and W.I. Wang, J. Vac. Sci. Technol. B **11**, 872 (1993).
7. D.L. Partin, J. Hermans, and C.M. Thrush, J. Vac. Sci. Technol. B **17**, 1267 (1999).
8. X. Weng, N.G. Rudawski, P.T. Wang, R.S. Goldman, D.L. Partin, and J. Heremans, J. Appl. Phys. **97**, 43713 (2005).
9. T.D. Mishima, J.C. Keay, N. Goel, M.A. Ball, S.J. Chung, M.B. Johnson, and M.B. Santos, J. Cryst. Growth **251**, 551 (2003).
10. T.D. Mishima, J.C. Keay, N. Goel, M.A. Ball, S.J. Chung, M.B. Johnson, and M.B. Santos, Physica E **20**, 260 (2004).
11. T.D. Mishima, J.C. Keay, N. Goel, M.A. Ball, S.J. Chung, M.B. Johnson, and M.B. Santos, J. Vac. Sci. Technol. B **23**, 1171 (2005).
12. J.W. Edington, *Practical Electron Microscopy in Materials Science*, (Van Nostrand Reinhold Company, 1976), p. 120.